JMEPEG (2010) 19:894–899
DOI: 10.1007/s11665-009-9559-7

1059-9495/$19.00

The Effect of Coating Thickness on Corrosion Resistance of Hydroxyapatite Coated Ti6Al4V and 316L SS Implants

B. Aksakal, M. Gavgali, and B. Dikici

(Submitted March 17, 2009; in revised form August 12, 2009)

Hydroxyapatite (HAP) has been coated onto Ti6Al4V and 316L SS substrates by sol-gel method. The coating thicknesses for the analysis were about 40 and 72 µm. Adhesion and corrosion tests have been conducted on uncoated and HAP-coated substrates. The coatings were characterized by XRD, SEM, and adhesion analysis. The corrosion resistance was examined in vitro by potentiodynamic polarization technique in Ringer's solution at room temperature. Electrochemical analysis indicated that the highest corrosion susceptibility was found on 72-µm-coated 316L SS, and the 40-µm HAP-coated Ti6Al4V showed the highest corrosion resistance. It was observed that the coating thickness was an effective parameter on both adhesion and corrosion resistance. It was shown that adhesion and corrosion resistance decreased with increasing coating thickness on both substrates.

Keywords biomaterials, coatings, corrosion, sol-gel

1. Introduction

Corrosion is a great concern, particularly, when a metallic implant is placed in hostile electrolytic environments such as in human body because the corrosion products have been implicated in causing infections, local pain, swelling, and loosening. It can, therefore, severely limit the fatigue life and ultimate strength of the material, leading to the in vivo failure of implants (Ref 1). The human body shows natural reaction against prosthetic devices causing the osteolysis and has the tendency to isolate from the surrounding live tissues. HAP coatings are applied to metallic implants to provide better osteointegration between bone and implant and the surface protection against body fluid. The ability of such HAP coatings helps to integrate implant to bone and support new bone generation (Ref 1). However, it is doubtful whether HAPs have enough stability in living body in the long term when exposed to wear, chemical attack, and to more load bearings during orthopedic applications. Therefore, the adhesion and corrosion resistance of HAP-coated implants were tested using the SBF for two different coating thicknesses, and only two thicknesses have been chosen for the analysis.

The metallic alloys used in orthopaedics for fabrication of artificial joints, undergo corrosion and release metallic ions into the patient's body. The release of corrosion products may elicit an adverse biological reaction in the host, and several authors have reported such corrosion-resistant products (Ref 2-5). Even stainless steels and Ti alloys are highly susceptible to corrosion in aggressive environments. Engineers and orthopaedics combine together to make an orthopedic patient's life to normal and provide a painless life when the prosthetic implants used. The most common corrosion resistant prosthetic devices are made of stainless steels and Ti alloy.

Surface films play key role in corrosion and osseointegration processes of implants. Numerous surface modifications of common alloy implants were performed to improve their corrosion resistance (Ref 3, 4). Urban et al. (Ref 5) showed that there is no histological evidence to slow metal release of species that assumed to occur in association with most metal implants, accelerated corrosion, and tissue response. Park and Lakes (Ref 6) showed that the products can cause local pain and swelling in implanted bodies. In general, very thin oxide films formed in aqueous environment also play a decisive role during sintering in determining the biocompatibility and corrosion behavior of the substrates. The increase in corrosion resistance is reported with increasing protection oxide layer thickness (Ref 7, 8) and many attempts were, therefore, made to form such oxide layers (Ref 9-11).

The wear and corrosion of the counterparts in sliding screw plates produce debrises (Ref 12-15). Furthermore, corrosion changes the chemical environment around the implant, inducing an acidic pH (Ref 16) and, thus, increasing the likelihood of corrosion. Surgically removed stainless steel hip screw plates showed significant wear, corrosion, and damage to the surrounding tissue (Ref 17). Similar study with implant alloys such as titanium and 316L steel (Ref 18-20) also supported these observations. Berger et al. (Ref 21) showed another failure case that occurred due to dissolution from HAP-coated implants. The corrosion performance of alumina-coated 316L SS was tested in Ringer's solution, and it was shown that a stable silica-alumina interface and enhanced corrosion protection was reported (Ref 22). Ducheyne et al. (Ref 23) studied to formulate and model the porous electrophoretic deposition (EPD) coatings. The deposition of ceramic coating can be hampered by adsorbed water and subsequent vacuum sintering leading to several phase transformations.

B. Aksakal, Department of Mechanical Education, Technical Education Faculty, Firat University, 23119 Elazig, Turkey; **M. Gavgali**, Department of Mechanical Engineering, Ataturk University, 25240 Erzurum, Turkey; and **B. Dikici**, Ercis Technical Vocational School of Higher Education, Yuzuncu Yil University, 65400 Van, Turkey. Contact e-mail: b.aksakal@firat.edu.tr.

These selected studies illustrate the number of variables involved in the implant failure and corrosion process. However, it is also important to see the effects of coating thickness on adhesion and corrosion that coated onto commonly used substrates via a fast and flexible dipping method. In this study, the effects of coating thickness on corrosion behavior of HAP-coated Ti6Al4V and 316L SS implants are examined by potentiodynamic polarization technique. Adhesion and corrosion tests have been carried out for two different thicknesses. The thinner (~40 μm) dip-coated implants showed higher bonding strength and corrosion resistance.

2. Materials and Methods

2.1 HAP Coating

The specimens were machined from the both Ti-6Al-4V alloy and 316L SS strips having the dimensions of $10 \times 10 \times 2$ mm. Before the sol-gel coating process, the substrates were sand blasted by silica beads with particle size of 50 μm. The metal substrates were thoroughly washed with a detergent, then ultrasonically cleaned twice with acetone for 30 min, and afterward passivated in nitric acid overnight. A novel sol-gel process is prepared and applied to Ti6Al4V and 316L SS substrates with controlled dipping and withdrawal rate for thinner and thicker HAP coatings. The coating thickness is varied, which is determined by adjusting the rate of soaking and removing back of the substrates from the gel. It involves simply preparing an adequate sol suspension by mixing HAP (Merck, Ca/P = 1.67) with Ethanol (%99.5) in a 250-mL grinding jar and milling it for 4 h and providing gel using a homogenizer, then by dipping the workpiece into the prepared sol-gel. In order to provide a fine and homogenized ceramic sol-gel, the biocompatible binder in the amounts of P_2O_5: 47 wt.%, Na_2CO_3: 20 wt.%, KH_2PO_4: 5 wt.% all purchased from Sigma-Aldrich are used. A dipping apparatus has been designed and manufactured allowing the substrate to be withdrawn with adjustable rates. Various thicknesses were fabricated in the thickness range of 10-100 μm; however, only two of them (40 and ~72 μm) were chosen for the adhesion and corrosion analysis.

Hydroxyapatite powders (Merck) having an average particle size of <5 μm are used. The mixture of ethanol (min 99.8%, Sigma-Aldrich) and HAP was blended continuously for 48 h in a grinder (Restch PM-400 at 300 rpm) resulting in very homogeneous and finer HAP particles (<1 μm) in the suspension. The homogenization suspension consisted of HAP (35 wt.%); few drops of glycerol (Merck), P_2O_5 (Sigma-Aldrich): 37 wt.%, Na_2CO_3 (Sigma-Aldrich): 20 wt.%, KH_2PO_4 (Sigma-Aldrich): (8 wt.%), and 25 mL distilled water are used (Ref 24). The produced sol was mixed and homogenized with those of additives in appropriate amounts in a 125-mL glass beaker using a 750-Watt ultrasonic processor with a temperature controller (Cole-Parmer) and a titanium probe with a tip diameter of 1/2". The ultrasonic treatment took place for 20 min, and a gel was obtained, having a viscosity of 22 cp. Ti substrates are coated with the thicknesses of ~40 and ~72 μm by dipping method and sintered in vacuum at temperature of 690 °C, and 316L SS substrates are sintered at 500 °C for 1.5 h. Since Ti induces the decomposition of HAP above 1050 °C (Ref 25, 26), the sintering temperatures were kept as low as possible in this study.

2.2 Pull-Out Test

Ti6Al4V and 316L strips were machined to have dimensions of $2 \times 10 \times 100$ mm and subjected to the same coating procedures explained above. Averages of six specimens were tested for two coating thicknesses and substrates, individually. The adhesive of FM 73 having 47 MPa bonding strength was subjected onto those coated surfaces and cured at 180 °C under a constant load of 5 kg for 2 h. Afterward, the pull-out tests were performed to those coated and adhered specimens under increasing load at a crosshead speed of 1.5 mm/min using a tensile test machine (Autograph AG-100kN, Shimadzu, Japan) until the shearing failure occurred. The films obtained from the prepared sol-gel method along with the FM 73 toughened epoxy (TAI, Turkish Aerospace Industries Inc.) were applied on one side of the coated surfaces (40 and ~72 μm) of the strips. The failure mode is recorded gradually, and the bonding strength is calculated as the load at failure divided by the coated bonded area. The highest bonding strength is calculated to be 17.1 MPa for Ti6Al4V, and 13.4 MPa for 316L substrates for the (~40μm) coating thickness on average.

2.3 Corrosion Tests

The corrosion behavior of HAP coatings and uncoated samples were investigated by potentiodynamic polarization technique. All the electrochemical measurements were carried out in accordance with ASTM standard of G5-94 (Ref 27). The electrochemical behaviors of the materials have been analyzed in deaerated Ringer's solutions (NaCl = 8.60 g/L, $CaCl_2.2H_2O$ = 0.33 g/L and KCl = 0.30 g/L) in a pyrex glass cell. The pH of the test solution was 5.73 at room temperature. The potentiodynamic polarization curves were obtained by an Ag/AgCl reference electrode and a platinum (Pt) counter-electrode. The exposed area of the working electrodes was about 1 cm^2. The corrosion tests were performed by using a Wenking PGS95 potentiostat (BANK). The solution was deaerated to remove oxygen with nitrogen (N_2), and the process was started 1 h prior to the measurement. The specimens were immersed into the solution until obtaining a steady open circuit potential (OCP). After equilibration, polarization started at a rate of 1 mV/s. The cycle began at the cathodic over potential according to OCP, and the scan was stopped when the specimens reached the anodic current density of approximately 1 mA/cm^2. After polarization, the examinations of the corroded surfaces were carried out by using a Leo type scanning electron microscope (SEM).

3. Results and Discussion

Hydroxyapatite was coated onto Ti6Al4V and 316L SS substrates by sol-gel method and adhered to the surface by the sintering effect. A variety of coating thicknesses were achieved whereas, here, only the (~40 μm) and (~72 μm) coating thicknesses were chosen for the adhesion and corrosion tests. The XRD results of the coated surfaces of Ti6Al4V and 316L substrates are shown in Fig. 1 and 2, respectively. The overall morphology of the coating surface is given in Fig. 3 at low magnification. The detailed surface morphologies after the coating process of the thinner (40 μm) HAP-coated and sintered surfaces are shown in Fig. 4 and 5. As seen in Fig. 4, a better network and interconnection of HAP powders is present on the coated surface morphology. Figure 5 shows the surface

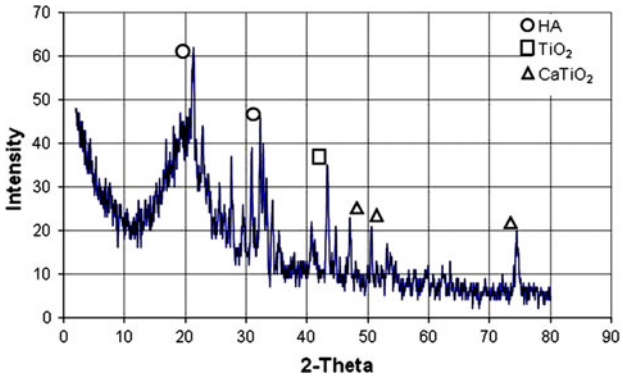

Fig. 1 XRD of coated and sintered Ti6Al4V surface

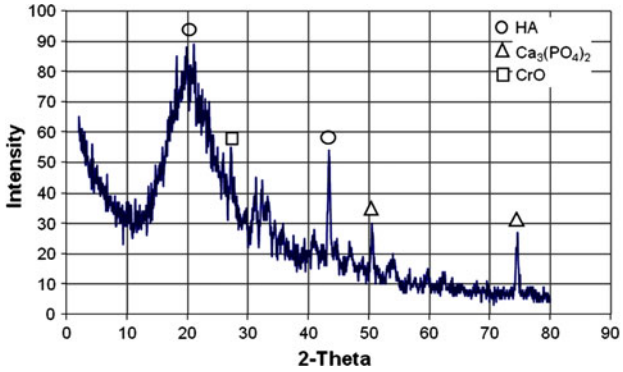

Fig. 2 XRD of coated and sintered 316L surface

morphology of the thicker coating (~72 μm). The bonding network is not that bad but not as good as in the case of thinner (~40 μm) coating (Fig. 4). It is observed that the thinner coating presents better interconnection between HAP powders than the thicker-coated (~72 μm) specimens. The adverse effects of implant-derived wear particles on periprosthetic tissues are also important that cause bone loss and likely lead to loosening effect between bone and implant. The loosening of implant is correlated to poor initial fixation and design, which is one of the major problems and principal causes of failure related to corrosion and wear of the prosthetic components (Ref 27, 28). The cross section of the HAP coating (~40 μm) of Ti6Al4V is shown in Fig. 6. It was observed that as the coating thickness increases, the surface cracks occur, and they reach to a significant level when the thickness is more than 40 μm, and such cracks may well cause to loosening of the implants.

The bonding of such ceramic coatings to the metallic implants is important, and they have been examined via pull-out tests for two coating thicknesses. The values of bonding strength for thicker coatings were found to be lower than that of thinner-coated ones. Bonding strength of HAP coatings decreased with increasing coating thickness. After the corrosion tests, it was observed that the bonding strength is reduced. More or less, the similar trends are present for 316L substrate as shown in Fig. 7(a). The bonding strength achieved in previous studies is between 14 and 20 MPa (Ref 1, 24) depending on the coating process and sintering temperature. The bonding strength in this study diminished to 11 MPa for ~72μm coating, whereas it was 13.4 MPa for ~40 μm coating, and even this still lowered after corrosion. As shown in Fig. 7(b), the bonding strength of ~40-μm coated and sintered Ti-6Al-4V

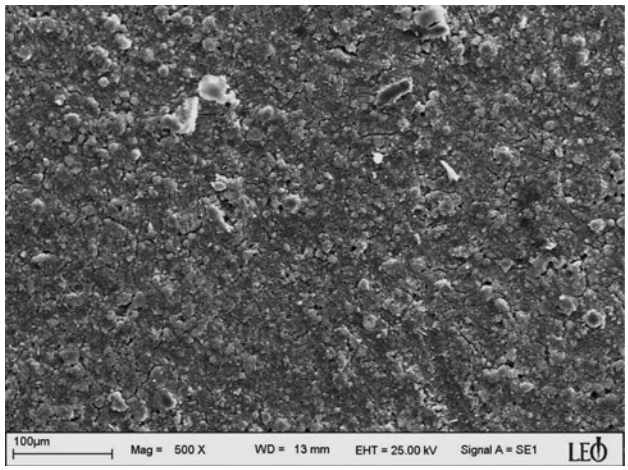

Fig. 3 The surface morphology of Ti6Al4V after the coating

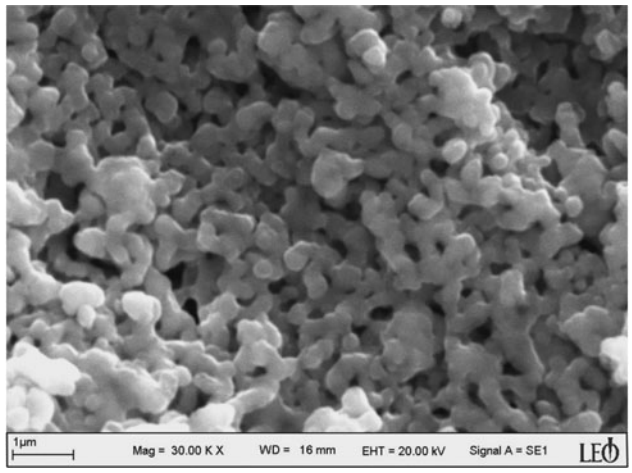

Fig. 4 SEM view of coated (~40 μm) and sintered Ti6Al4V substrate before corrosion

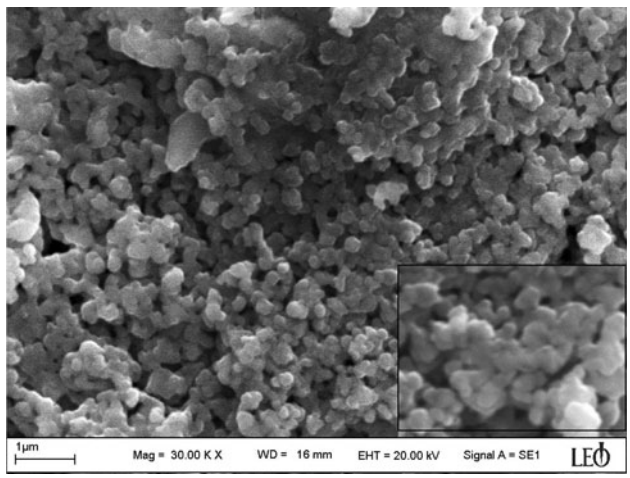

Fig. 5 SEM view of coated (~72 μm) and sintered Ti6Al4V substrate before corrosion

surface is found to be 17.1 MPa; however, it reduced to 16.2 MPa for ~72 μm coating, and the rest of coatings showed nearly similar trends. On comparison of both substrates,

Fig. 7(a) and (b), better bonding can easily be seen for Ti6Al4V. Some of the coatings, especially at excessive thick coatings (>40 μm, 316L) exhibited more surface cracks than that of thinner ones after drying and sintering process. The substrates have to be immersed in a prepared sol-gel; then, dipping process should take place to get crack-free surfaces. However, through this study, first, the optimum coating parameters were determined, and then, the dipping process was performed to the specimens. The conjoint degradation processes of corrosion and wear of metal surfaces is clearly of great importance in the design of orthopedic prostheses. However, during the overall degradation when both corrosion and wear processes took place, the results showed that the corrosion resistance was highest for Ti-6Al-4V (Ref 18). The clinical consequences of at least partially corroding implants are well known. The release of solutes, i.e., the corrosion products, at an implant site may cause histologic changes in the local tissue by either direct toxic effect or a local hypersensitivity reaction (Ref 29).

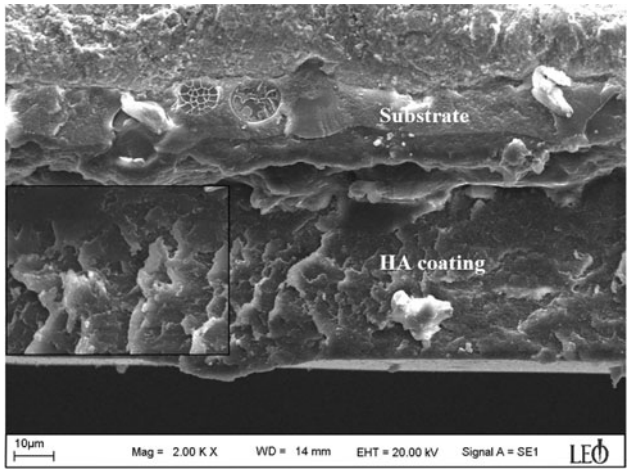

Fig. 6 Cross section of HA coating (~40 μm) of Ti6Al4V

The potentiodynamic polarization tests were undertaken in Ringer's solution, and the related curves of thin and thick HAP-coated and -uncoated specimens, in comparison, are given in Fig. 8. All these curves exhibit a similar regime for the base materials, but the E_{corr} and E_{pit} values of the coated materials were reproducible in the variation of ±15 mV. The most critical parameters such as corrosion potential (E_{corr}), pitting potential (E_{pit}), and current density (i_{corr}) values obtained from this curves are summarized in Table 1. It can

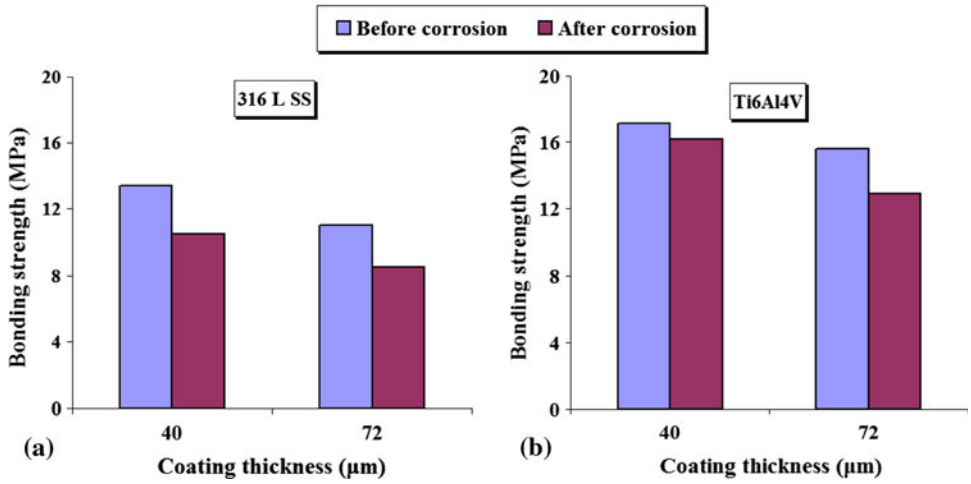

Fig. 7 Variation of bonding strength with coating thickness (a) 316L and (b) Ti6Al4V

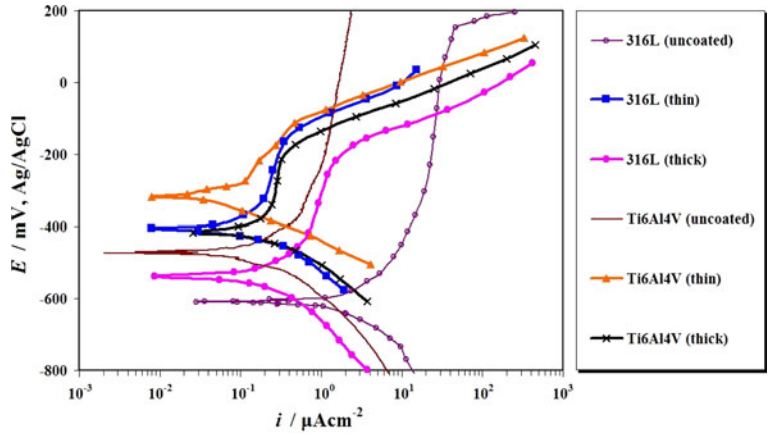

Fig. 8 Potentiodynamic polarization curves of the HA-coated materials and substrates specimens in Ringer's solution

Table 1 Corrosion (E_{corr}), pitting (E_{pit}) potentials and current density (i_{corr}) values of the HA-coated and uncoated implants in deaerated Ringer's solution

Substrate	Surface treatment	E_{corr}, mV	E_{pit}, mV	i_{corr}, μA/cm^2	i_{pass}, μA/cm^2
316L	Uncoated specimen	−609	137	5.15	11.00
	~72 μm HAPcoated	−537	−216	0.35	0.95
	~40 μm HAPcoated	−405	−165	0.10	0.20
Ti6Al4V	Uncoated specimen	−473	…	0.18	0.95
	~72 μm HAPcoated	−416	−213	0.25	0.35
	~40 μm HAPcoated	−317	−112	0.05	0.15

be clearly seen from Fig. 8 and Table 1 that the highest corrosion resistance was exhibited by the thinner HAP coated over the Ti6Al4V specimens in the Ringer's solution at room temperature. In addition, the E_{corr} values of the specimens increase negatively with increasing HAP-coating thickness; for example, for Ti6Al4V specimen, it is measured to be ~90 mV which is higher than the thinner HAP-coated 316L specimen (−405 and −317 mV for thinner HAP-coated 316L and Ti6Al4V specimens, respectively). In other words, the corrosion potential of the thinner HAP-coated Ti6Al4V specimen is more noble than thinner HAP-coated 316L SS.

According to Galvele (Ref 30), corrosion current is the intersection between the anodic and cathodic linear extrapolations at E_{corr}. The value is directly related to electrode potential, and it can be provide more realistic results related to the electrochemical behavior of the material. The current density value is directly related to the electrode potential; thus, E_{corr} and i_{corr} values can provide more realistic results related to electrochemical behavior of the implants (Ref 30). From the inspection of polarization curves given in Fig. 8, the passivity (i_{pass}) and current density values (i_{corr}) decrease with decreasing HAP layer thickness, provided that the corrosion takes place at a lower rate for the thinner HAP-coated implants. The lowest i_{corr} values were calculated as 0.1 and 0.05 μA/cm^2 for the thinner HAP-coated 316 L SS and Ti6Al4V implants, respectively. These results are in good agreement with galvanic series of metals because it is well known that the corrosion potential of 316L SS is typically more active than Ti alloys (Ref 31, 32). The increased currents would occur if the metal dissolves from the substrate and precipitates as hydrated salts on its surface which has been claimed to result in enhanced corrosion resistance of the underlying substrate (Ref 25). The decrease in the value of breakdown potentials with the increase in coating thickness can be attributed to the porosity and surface energy. The likely mechanism for low corrosion resistance of 316L SS may be attributed to the deagglomeration, accompanied by the subsequent interparticle fissure formation of particles and eventual particle detachment from the substrate (Ref 33). It is evident, from the results presented, that compared to HAP-coated 316L SS, the thinner HAP-coated Ti6Al4V exhibit enhanced E_{pit} and E_{corr} values, suggesting an improvement in the pitting corrosion resistance.

In vitro polarization corrosion test results indicate that the release of metallic ions for both thinner Ti6Al4V and 316L SS coatings decrease and so deleterious effects on body tissues therefore may offer desired properties such as biocompatibility, bonding and osseointegration capabilities and so presumably prevent the tissues from inflammations and irritations. The thinner HAP coating is preferable in prosthetic devices and in this work, on the contrary to a few previous works (Ref 7-11) stating the thin hydroxyapatite coatings below about 50 μm will be rather quickly resorbed. In the present study, the thinner dip-coated implants showed higher corrosion resistance. The reason for this could well be because of the occurrence of severe surface cracks on thick coatings over about 40 μm and this causing the easy contact of implant surface with the corrosive liquid and that diminishes the corrosion resistance. In addition it is also observed that the porosities increase with increasing coating thickness (Fig. 4 and 5). The porosities existing on the coated surface are the areas where the electrolyte (ringer's solution) is stagnating and because of this, oxygen transfer becomes difficult. By increasing the potential, these porosities are intended to be filled up with corrosion products and passivate the upper surface. Thus, porosities of the coating will act as preferential corrosion areas. In the other words; increasing the coating thickness increases the level of porosities and microcracks where corrosion can be initiated and so rendering the HAP coating liable to severe attack (Fig. 9).

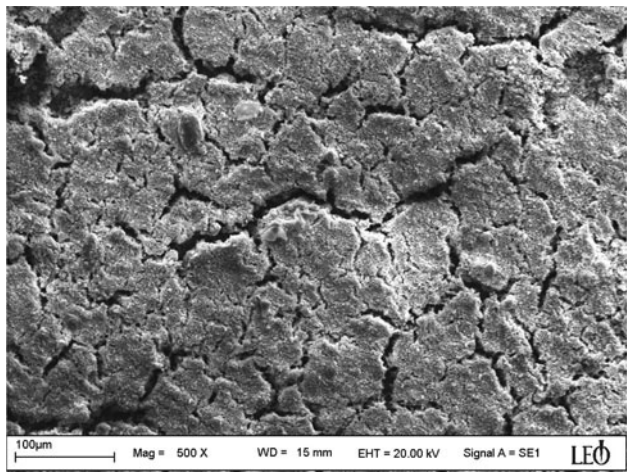

Fig. 9 SEM micrograph of thin-coated Ti6Al4V after corrosion test

The effect of important parameters such as particle size, characterization, and crystallization of the coating powder were reported previously (Ref 1, 23, 24, 34, 35). The as-sputtered coatings are usually non-stoichiometric and amorphous, which can cause some serious problems such as poor adhesion and excessive coating dissolution rates (Ref 18, 22, 23). Using the dip-coating method, it was observed that the current HAP coatings are stoichiometric, and crystalline as evidenced by XRD, and strongly bonded to the substrate (as high as 21 MPa). In particular, coatings deposited on oriented substrates show a polycrystalline XRD pattern, but with some strongly preferred orientations indicating that HAP crystallization is sensitive to the nature of the used substrates.

4. Conclusions

Hydroxyapatite (HAP) has been successfully deposited onto Ti6Al4V and 316L stainless steel substrates by sol-gel method. The bonding strength was determined via pull-out tests, and 17.1 MPa was achieved for the 40 μm of coating on Ti6Al4V alloy. The optimum coating and sintering parameters were determined, and surfaces were characterized through XRD and SEM. The corrosion resistance of the uncoated and coated implants was evaluated in comparison with two different thicknesses via polarization tests. The thinner HAP-coated Ti6Al4V samples exhibit the most enhanced corrosion parameters (E_{corr}, E_{pit}, i_{corr}) and thus suggesting an improvement in the corrosion resistance of the material. In brief, these results showed that there is a significant correlation between corrosion susceptibility and HAP coating thickness, but it is necessary to test such coatings over longer periods in in vitro and in vivo examinations before using them in live body.

References

1. O.S. Yildirim, B. Aksakal, H. Celik, Y. Vangolu, and A. Okur, An Investigation of the Effects of Hydroxyapatite Coatings on the Fixation Strength of Cortical Screws, *J. Med. Eng. Phys.*, 2005, **27**(3), p 221–228
2. V. Pasekova, Z. Klezl, K. Balik, and M. Adam, Biomechanical and Biological Properties of the Implant Material Carbon-Carbon Composite Covered with Pyrolytic Carbon, *J. Mater. Sci.: Mater. Med.*, 2000, **11**, p 793–798
3. U.E. Pazzaglia, C. Minoia, G. Gueltieri, I. Gueltieri, C. Riccardi, and L. Ceccilliani, Metal Ions in Body Fluids After Arthroplasty, *Acta Orthop. Scand.*, 1986, **57**, p 415–418
4. L.D. Dorr, R. Bloebaum, J. Emmanual, and R. Meldrum, Histologic, Biochemical and Ion Analysis of Tissue and Fluids Retrieved During Total Hip Arthroplasty, *Clin. Orthop.*, 1990, **261**, p 82–95
5. R.M. Urban, J.J. Jacobs, J.L. Gilbert, and J.Q. Galante, Migration of Corrosion Products from Modular Hip Prosthesis: Particle Microanalysis and Histopathological Findings, *J. Bone Joint Surg.*, 1994, **76**(A), p 1345–1359
6. J.B. Park and R.S. Lakes, *Metallic Implant Materials in Biomaterials: An Introduction*, Plenum press, NY, 1992, p 75–115
7. M. Cabrini, A. Cigada, G. Rondelli, and B. Vicentini, Effect of Different Surface Finishing and Hydroxyapatite Coatings on Passive and Corrosion of Ti6Al4V Alloy Simulated Physiological Solution, *Biomaterials*, 1997, **18**, p 783–787
8. R. Brown, M.N. Alias, and R. Fontana, Effect of Composition and Thickness on Corrosion Behaviour of TiN and ZrN Films, *Surf. Coat. Technol.*, 1993, **62**, p 467–473
9. H. Ishizawa and M. Ogino, Formation and Characterization of Anodic Titanium Oxide Films Containing Ca and P, *J. Biomed. Mater. Res.*, 1995, **29**, p 65–72
10. I. Vaquila, L.I. Vergara, J.R. Passeggi, R.A. Vidal, and J. Ferron, Chemical Reactions at Surfaces: Titanium Oxidation, *Surf. Coat. Technol.*, 1999, **122**, p 67–71
11. D.B. Haddow, S. Kothari, P.F. James, R.D. Short, P.V. Hatton, and R. van Noort, Synthetic Implant Surfaces: The Formation and Characterization of Sol-Gel Titania Films, *Biomaterials*, 1996, **17**, p 501–507
12. J.L. Gilbert, C.A. Buckley, et al., Intergranular Corrosion-Fatigue Failure of Cobalt-Alloy Femoral Stems, *J. Bone Joint Surg.*, 1994, **76**(1), p 110–115
13. W.L. Jaffe and D.F. Scott, Total Hip Arthroplasty with Hydroxyapatite-Coated Prosthesis, *J. Bone Joint Surg.*, 1996, **78**(A12), p 1919–1934
14. D.W. Howie, S.D. Rogers, et al., Biological Effect of Cobalt Chrome in Cell and Animal Models, *Clin. Orthop.*, 1996, **329S**, p 217–232
15. M.M. Edwin, V.A. Edward, J.S. Peter, and J.S. Neal, Exchange Nailing for Failure of Initially Rodded Tibial Shaft Fractures, *J. Orthop.*, 2001, **24**(8), p 757–762
16. H.G. Willer, L.G. Broback, and G.H. Buchorn, Crevice Corrosion of Cemented Titanium Hip Implants, *Clin. Orthop.*, 1996, **333**, p 51–57
17. B.F. Shagaldi and J. Compson, Wear and Corrosion of Sliding Counterparts of Stainless-Steel Hip Screw-Plates, *Injury Int. J. Care Injured*, 2000, **31**, p 85–92
18. M.A. Khan, R.L. Wiliams, and D.F. Williams, Conjoint Corrosion and Wear Titanium Alloys, *Biomaterials*, 1999, **20**, p 765–772
19. L. Reclaru, et al., Corrosion Behaviour of a Welded Stainless-Steel Orthopedic Implant, *Biomaterials*, 2001, **22**, p 269–279
20. J. Walczak, F. Shahgaldi, and F. Heatley, In Vivo Corrosion of 316L Stainless-Steel Implants, *Biomaterials*, 1998, **19**, p 229–237
21. G. Berger, U. Ploska, and G. Willmann, Hydroxyapatite's Solubility May Cause Loosening of Coated Implants, *Proceedings of the 13th Int Symp on Ceramics in Medicine*, Bologna, Italy, 2001, p 192–195
22. S.K. Tiwari, T. Mishra, M.K. Gunjan, A.S. Bhattacharyya, T.B. Singh, and R. Singh, Development and Characterization of Sol-Gel Silica-Alumina Composite Coatings on AISI, 316L for Implant Applications, *Surf. Coat. Technol.*, 2007, **201**, p 7582–7588
23. P. Ducheyne, S. Radin, M. Heughebaert, and J.C. Heughebaert, Calcium Phosphate Ceramic Coatings On Porous Titanium: Effect of Structure and Composition on Electrophoretic Deposition, Vacuum Sintering and In Vitro Dissolution, *Biomaterials*, 1990, **11**, p 244
24. B. Aksakal and C. Hanyaloglu, Bioceramic Dip-Coating on Ti-6Al-4V and 316L SS Implant Materials, *J. Mater. Sci.: Mater. Med.*, 2008, **19**, p 2097–2104
25. T.M. Sridhar, U.K. Mudali, and M. Subbaiyan, Preparation and Characterization of EPD Hydroxyapatite Coatings on Type 316L SS, *Corros. Sci.*, 2003, **45**, p 237–252
26. G. Haicheng, G. Huifang, C. Shufen, and C. Laird, Orientaiton Dependence of Cyclic Deformation in High Purity Titanium Single Crystals, *Mater. Sci. Eng. A*, 1994, **118**, p 23–36
27. ASTM G1-94, ASTM Int., 2001, p 58–69
28. A.M. Gee Margaret, et al., Implant Retrieval Studies of the Wear and Loosening of Prosthetic Joints: A Review, *Wear*, 2000, **241**, p 158–165
29. I. Aitchison and B. Cox, Interpretation of Fractographs of SSC in hexagonal metals, *Corrosion*, 1972, **28**(3), p 83–87
30. J.R. Galvele, Tafel's Law in Pitting Corrosion and Crevice Corrosion Susceptibility, *Corros. Sci.*, 2005, **47**, p 3053–3067
31. S. Kannan, A. Balamurugan, and S. Rajeswari, Hydroxyapatite Coatings on Sulfuric Acid Treated Type 316L SS and Its Electrochemical Behaviour in Ringer's Solution, *Mater. Lett.*, 2003, **57**, p 2382–2389
32. S. Kannan, A. Balamurugan, and S. Rajeswari, Electrochemical Characterization of Hydroxyapatite Coatings on HNO3 Passivated 316L SS for Implant Applications, *Electrochem. Acta*, 2005, **50**, p 2065–2072
33. S. Suresh, *Fatigue of Mater*. Cambridge University Press, New York, 1998
34. A.C. Tas, Synthesis of Biomimetic Ca-Hydroxyapatite Powders at 37 °C in Synthetic Body Fluids, *Biomaterials*, 2000, **21**(14), p 1429–1438
35. A.C. Tas, F. Korkusuz, M. Timucin, and N. Akkas, An Investigation of the Chemical Synthesis and High-Temperature Sintering Behaviour of Calcium Hydroxyapatite (HA) and Tricalcium Phosphate (TCP) Bioceramics, *J. Mater Sci: Mater. Med.*, 1997, **8**, p 91–96